Synthesis and Characterization of Copper Oxide Nanoparticles and Investigation of their Catalytic Effect on Thermal Decomposition of Composite Propellants

By

Qasim Hassan Kazmi

School of Chemical and Materials Engineering

National University of Sciences and Technology

2018

Synthesis and Characterization of Copper Oxide Nanoparticles and Investigation of their Catalytic Effect on Thermal Decomposition of Composite Propellants

Name: Qasim Hassan Kazmi

Reg.No: NUST201463901MSCME67614F

This thesis is submitted as a partial fulfillment of the requirements for the degree of

MS in Energetic Materials Engineering

Supervisor Name: Dr. Abdul Qadeer Malik

School of Chemical and Materials Engineering (SCME)

National University of Sciences and Technology (NUST),

H-12, Islamabad, Pakistan

June, 2018

Dedicated to my Parents

Acknowledgments

All thanks to Allah for all of His countless blessings upon me and peace, blessings and salutations upon His last and beloved Prophet, Hazrat Muhammad (PBUH).

I would like to acknowledge and express my sincere gratitude to my research supervisor, Dr. Abdul Qadeer Malik for his best support, supervision and affectionate guidance to steer me in the right direction whenever he thought I needed it. Thanks and gratitude to my guidance committee members; Dr. Arshad Hussain and Dr. Habib Nasir for their valuable suggestions and guidance.

I am thankful to my teacher Col® Nadeem Ehsan who has been very affectionate and supportive for the accomplishment of this task. Special thanks to Mr., Muhammad Ali, a visiting faculty from POF Wah Cantt. for all his support and guidance. Thanks are also extended to Dr. Sarah Farrukh, Dr. Ahmed Nawaz Khan, Dr. Taqi Mehran and all faculty and staff of SCME for their support and direction.

I am indebted to my class fellows: Mr. Junaid Akhtar, Mr. Shah Faisal for their nice and pleasant company at NUST, Islamabad.

Special thanks to my seniors and colleagues especially Mr. Khalil ur Rahman, Mrs. Dilshad Kosar, Mr. Absaar Muhammad Yusaf, Mr. Muhammad Saqib, Dr. Naveeda Firdous, Mr. Imran Haider, Mr. Bilal Farooqi, Hafiz Abdul Raheem and Mr. Abdul Rehman for their cooperation during my thesis work.

I pay my homage and sweet sensation of love and respect to my family: Saman, Abbas and Hussain. It would not have been easy without their cooperation and prayers to attain this target.

Qasim Hassan Kazmi

Abstract

Copper oxide (CuO) nanoparticles were prepared by sol-gel and thermal decomposition method. In this technique, copper (II) sulfate pentahydrate ($CuSO_4.5H_2O$) is added with sodium carbonate (Na_2CO_3) by constant stirring and heating to produce green precipitates. The precipitates were filtered, washed with warm deionized water and dried. Thermal decomposition of precipitates is carried out in muffle furnace to produce black nanoparticles of CuO. The composition, structure and morphology of the prepared CuO nanoparticles were characterized using Fourier transform infrared (FTIR) spectroscopy, X-Ray diffraction (XRD) and scanning electron microscopy (SEM) respectively. FTIR spectrum revealed absorption peaks at 480-585 cm^{-1} due to the vibrations of Cu (II)-O bonds. The XRD pattern was well matched with the monoclinic phase of CuO (tenorite) and well consistent with ICDD File # 05-0661. The average crystallite size of CuO nanoparticles was calculated by using Debye Sherrer equation and found equal to 63.3 nm. The morphology of CuO nanoparticles was examined by SEM images at different resolutions and cylindrical shaped nanoparticles were observed.

CuO nanoparticles were mixed with composite propellant to investigate its effects on thermal decomposition of composite propellant. Composite propellant was composed essentially of ammonium perchlorate (AP) as oxidizer and hydroxyl terminated polybutadiene (HTPB) as binder. Thermo gravimetric (TG) analysis and differential thermal gravimetry (DTG) of composite propellant mixed with 1%, 2% and 3% of CuO were performed. Descending trend in decomposition temperature of composite propellant was observed by increasing the percentage of CuO nanoparticles. By mixing 3% CuO nanoparticles, 15˚C decrease in thermal decomposition temperature of composite propellant was observed.

Table of Contents

List of Figures

List of Tables

Abbreviations

A^o	Angstrom (10^{-10} m)
AN	Ammonium nitrate
AP	Ammonium perchlorate
^oC	Degree celsius
cm^{-1}	Per centimeter
CuO	Copper oxide
CMCDB	Composite modified cast double base
CDB	Cast double base
DTG	Differential thermogravimetry
DTA	Differential thermal analysis
DSC	Differential scanning calorimetry
EMCDBP	Elastomer modified cast double base propellant
FTIR	Fourier transform infrared
g/cm^3	Gram per cubic centimeter
GCMS	Gas chromatography–mass spectrometry
HTPB	Hydroxyl terminated polybutadiene
IRFNA	Inhibited red fuming nitric acid
I_s	Specific impulse
ICDD	International center of diffraction data
ICTA	International confederation of thermal analysis
JCPDS	Joint committee on powder diffraction standards
kJ $mole^{-1}$	Kilo joule per mole

log	Logarithm
ms^{-1}	Meter per second
NaOH	Sodium hydroxide
nm	Nanometer
$Ns\ kg^{-1}$	Newton second per kilogram
PVC	Polyvinylchloride
PIB	Polyisobutene
PU	Polyurethane
PBAN	Poly butadiene acrylic acid acrylonitrile
TG	Thermogravimetry
UDMH	Unsymmetrical dimethylhydrazine
USA	United States of America
3D	Three dimensional
%	Percent
θ	Theeta
λ	Lambda

Chapter 1

Introduction

1.1. Definition of nanomaterials

The term nano in the SI unit means 10^{-9}, or in words, one billionth. All the materials with as a minimum one dimension shorter than 100 nm is referred to as nanodimensional.

In year 2004, the United States National Nanotechnology Initiative (US NNI) defined nanomaterials as: “materials with dimensions of roughly 1-100 nm, where unique phenomenon enable novel application” [1].

According to the definition by European commission in 2011, the nanomaterials should have one or more dimension between 1 to 100 nanometer ranges or their specific surface area by volume should be more than 60 m^2/cm^3. The definition in terms of surface area does not include materials with particle size less than one nanometer. [1]

It is also defined that the materials that fall in the size range of nanomaterials, according to the above quoted definitions, must possess as a minimum one property clearly different from the larger size particles of the same material. [2]

1.2 Classification of nanomaterials

Nanoparticles can be classified as following three types:

1.2.1 Zero-dimensional nanomaterials

0-D nanoparticles are lesser than 100 nm in all directions. For example nanoparticles & nanopores. Such sort of nanomaterials is shown as Figure 1.1 (a).

1.2.2 One-dimensional nanomaterials

1-D nanomaterials are shorter than 100 nm in two directions only. Examples for 1-D nanomaterials are nanorods, nanowires, nanotubes etc. Such type of nanomaterials is shown as Figure 1.1 (b).

1.2.3 Two-dimensional nanomaterials

2-D nanomaterials are shorter than 100 nm only in a single direction. Examples for 1-D thin films, nano plates, graphene etc. as shown in Figure 1.1 (c).

1.2.4 Three-dimensional nanomaterials

3-D Nanomaterials are structures made up by joining together of nanomaterials. Such class of nanomaterials is shown as Figure 1.1 (d).

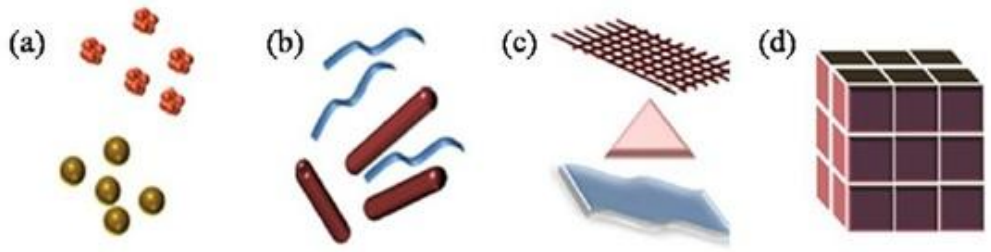

Figure 1. 1 Classification of nanomaterials

1.3 Applications of nanomaterials

At nano scale, the properties of materials like electrical, mechanical, optical and magnetic properties are usually altered as compared to the bulk of the materials. This change in properties is employed in many industries for the improvement of quality of end product. Some practical examples of uses of nanomaterials are as listed below:

- Nanophase ceramics are more ductile and able to be deformed without losing toughness at high temperatures as compared to larger size grained ceramic materials. Nanophase ceramic in the form of Nano-hydroxyapatite is also used as a bone substitute [3].
- Nanomaterials are also used in sports goods. Nanoparticles of carbon are being employed in the manufacturing of head and shaft of racquet (or racket) used in squash, tennis and badminton to improve its strength with less weight. Carbon nanotube epoxy matrix is also used in hockey sticks to make it stronger [4].
- Nanostructured semiconductors are used in electronic devices and sensors [5].
- Nanomaterials are utilized in automobile paints to improve its scratch-resistant property. Waxes made up of nanoparticles are used in automobile paints to improve its shining ability [6].

- Nanoemulsion technology is employed in the synthesis of nonflammable, noncorrosive and nontoxic antibacterial cleanser that is able to kill bacteria [7].
- Silver has the property of being antibiotic and is utilized in the treatment of wounds and burns. With nanoparticles of Silver, particular dressings are prepared for burns to offer added antimicrobial barrier protection [8].
- Non stain nanotechnology apparel fabric is introduced by several clothing companies that repels liquids like beverages and salad dressings [9].
- Nanoparticles like nano zinc oxide are being used by cosmetic companies for products like sunscreen, deodorants and antiaging cream [10].
- Nanomaterials have also found application in environmental problems solutions. For example, removal of radioactive ions from water, clean up of oil spills can be done by the use of nanomaterials [11].

1.4 Synthesis of nanomaterials

Synthesis of nanomaterials is performed mainly by two approaches as followings:

1.4.1 Top down approach

In the “top down” approach, nanomaterials are prepared from larger size objects to nano scale materials without atomic level control. Examples of such approach are attrition and milling methods for the preparation of nanomaterials.

1.4.2 Bottom up approach

Smaller entities are brought together chemically in bottom up approach to form nanoparticles. The main principle behind bottom approach is molecular recognition. One of the practical examples of bottom up approach in nanotechnology is colloidal dispersion. The concept of top down and bottom up tactic is also demonstrated by Figure: 1.2.

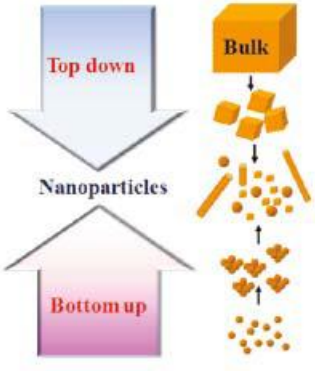

Figure 1. 2 Top down and bottom up approach

1.4.3 Synthesis techniques for nanomaterials

Few of the techniques used for the preparation of nanomaterials are as listed below:

- Mechanical grinding
- Sol gel process
- Gas phase synthesis of nanomaterials
- Furnace
- Flame assisted ultrasonic spray pyrolysis
- Gas condensation processing (GPC)
- Chemical vapor condensation (CVC)
- Sputtered plasma processing
- Microwave plasma processing
- Laser ablation

1.5 Characterization of nanomaterials

Some of the most common characterization techniques in nanotechnology are listed below:

- Electromagnetic spectroscopy
- Nuclear magnetic resonance (NMR) spectroscopy
- X-Ray photoelectron spectroscopy (XPS)
- X-Ray diffraction techniques (XRD)
- Fourier transform infrared (FTIR) spectroscopy
- Light scattering techniques
- Raman spectroscopy
- Scanning electron microscope (SEM)
- Transmission electron microscope (TEM)
- Scanning transmission electron microscope (STEM)
- Rutherford backscattering spectrometry (RBS)
- Scanning probe microscopy (SPM)
- Scanning tunneling microscope (STM)

Fourier transform Infrared (FTIR) spectroscopy, X-Ray diffraction (XRD) and scanning electron microscope (SEM) characterization are discussed in detail in

chapter 3 of this thesis report.

1.6 CuO nanoparticles

Copper oxide (CuO) or cupric oxide is a black solid inorganic compound and as a mineral it is also called tenorite.

1.6.1 Applications of CuO nanoparticles

Nanoparticles of CuO found applications in many industries. Few of the examples are listed below:

- CuO nanoparticles find application as catalyst to improve burning rate of propellants [12].
- CuO nanoparticles are employed in lithium ion batteries [13].
- CuO nanoparticles are used in magnetic storage devices [14].
- CuO nanoparticles are used in semiconductors [15].
- CuO nanoparticles are used in gas sensors [16].
- CuO nanoparticles are used in solar energy conversion [17].
- CuO nanoparticles are used in electrode material [18].
- CuO nanoparticles are used in super hydrophilic materials [19].
- CuO nanoparticles are used in high tech superconductors [20].

1.7 Rocket propellants

Rocket propellants are low explosives that are produced to burn efficiently deprived of the hazard of detonation to provide propulsive energy" [21]. Rocket propellants are similar to gun propellants in composition but due to difference in operating conditions and requirements, there are differences in formulation. The performance of rocket is highly dependent on the velocity when all the propellant is burnt and its maximum range. Specific impulse (I_s) is ratio of thrust to motor mass flow rate. The unit for specific impulse is Newton second per kilogram ($Ns\ kg^{-1}$) or simply meter per second (ms^{-1}).

1.7.1 Liquid propellants

Liquid propellants are of two types:

- Monopropellant

- Bipropellants

1.7.1.1 Liquid monopropellant

There is only one component present in liquid monopropellants. Liquid monopropellant undergoes spontaneous decomposition with the production of heat energy and volume of gas. In some cases, decomposition of liquid monopropellants just need a thermal energy source. But in certain cases an additional catalyst is required for decomposition of monopropellant. The specific impulse value of monopropellants is low as for Hydrazine its value is only 1950 ms^{-1}. Hydrazine is used as liquid monopropellant in attitude control thrusters in the existence of 30 percent iridium supported alumina catalyst. Other examples of some of the monopropellants are hydrogen peroxide & nitrous oxide etc.

1.7.1.2 Liquid bipropellant

In liquid bipropellant system, fuel and oxidizer are used separately. There are further two classes of liquid bipropellants system, hypergolic and non-hypergolic. In case of hypergolic liquid bipropellants, when fuel and oxidizer are injected in combustion chamber, spontaneous reaction takes place. Whereas an additional igniter is needed to start the reaction for non- hypergolic bipropellants. Example of liquid bipropellant system are listed below:

- Liquid hydrogen as fuel and liquid oxygen as oxidizer
- Hydrazine as fuel and nitrogen tetroxide as oxidizer etc.

1.7.2 Solid propellant

In case of solid propellant rockets, the rocket motor contains all the propellant inside the combustion chamber. The burning is inhibited on outside surface of grain by either boning the propellant grain to motor casing (case-bonded) or by applying flame resistant material on the outer surface of grain (Inhibited). Other than motor design and propellant grain shape, performance of solid propellant depends on following factors:

- Chemical and thermal stability
- Burning characteristics
- Mechanical strength etc.

Different shapes or cross sections of solid propellant grain for rocket motors are shown in figure below:

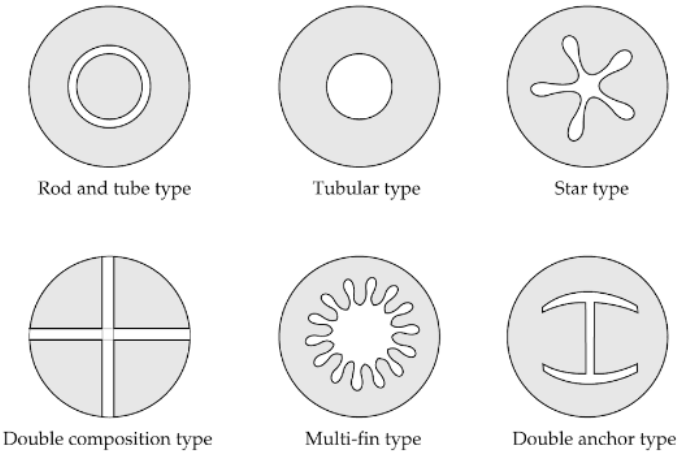

Figure 1. 3 Different shapes of solid propellant grain [22]

1.8 Types of solid propellant

To cover different features of solid propellant for various tasks, solid propellants are divided in three different classes.

- Double base
- Modified double base
- Composites.

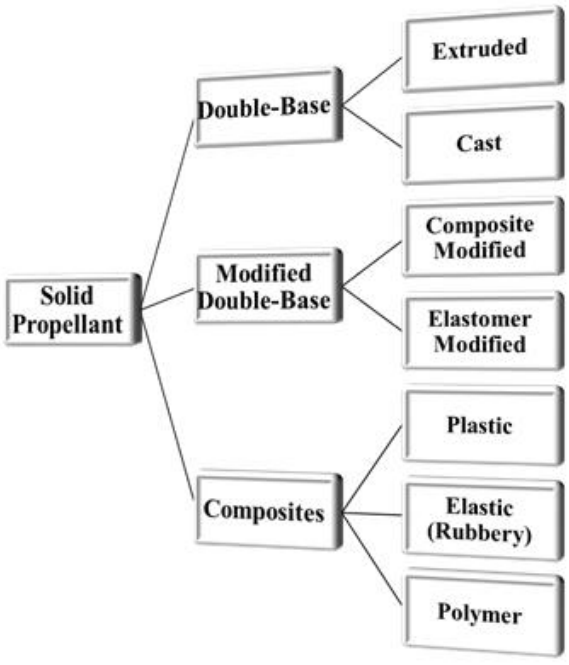

Figure 1. 4 Classification of solid propellants

1.8.1 Double-Base solid propellant

Double-base solid propellant generally are composed of nitrocellulose and nitroglycerine. An additional stabilizer is added in the composition to eliminate oxides of nitrogen that are produced by slow decay during storage. The removal of oxides of nitrogen is necessary because they can cause short storage life of propellant. Ethyl centralite is usually used as stabilizer in double base solid propellants.

Other additives in double base propellants include:

- Diethylphthalate is added as plasticizer to improve extrusion and avoid cracking.
- Potassium Sulfate is added as burning performance modifier.
- Wax is applied as die lubricant.
- Carbon black is employed to avoid radiated heat from the burning surface that can cause surface ignition before time.

Double base solid propellants are manufactured by two different methods i.e., extrusion and casting. The extrusion method is limited to grain diameter of maximum 13 centimeters with specific impulse value of up to 2300 ms^{-1}. For higher grain diameters, casting method is used for manufacturing. Double base solid propellant made by casting method contains higher percentage of nitrocellulose than extruded type. However specific impulse (I_s) in case of casting method is lowered to 2000 ms^{-1} as compared to extrusion method.

1.8.2 Modified Double-Base solid propellant

The specific impulse (I_s) of double base propellant can be increased by adding aluminum powder and oxidant such as ammonium per chlorate to cast double base composition. After addition of these ingredients, the resultant composition is called composite modified cast double base (CMCDB). They are also termed as filled CDBs. Further increase in performance is possible by the addition of nitramine such as HMX. A specific impulse value of 2600 ms^{-1} is possible with such composition.

CMCDBs are examples of hybrid rocket propellants. One of the problems of CDBs is low temperature cracking. IMI Summerfield Limited of United Kingdom has developed a further hybrid type that is called elastomer modified cast double base propellant (EMCDBP). In case of EMCDBPs, the object is to enhance the physical

properties such as extensibility of double base cast propellant. In such type of composition, an elastomeric polymer is added to the colloidal matrix to enhance low temperature strain capabilities.

1.8.3 Composite solid propellant

A composite propellant, in weight percentage, contains 10 to 15% polymer or binder. The presence of this binder improves the mechanical properties and it develops elastomeric property in propellant during the expansion and contraction due heating and cooling cycle within motor case. The elastomeric property of composite propellants helps to avoid detachment of propellant grain from motor case and keeps the case bonded with grain.

1.8.3.1 Binder for composite propellant

The usual prerequisite for a good binder are as follows:

- High tensile and compressive strength with excellent elasticity.
- Handy to accept a high solids loading and be suitable for manufacturing processes.
- Initially in liquid state with viscosity of 1-10 Nsm^{-2} that transfers to a solid on either cooling or curing.
- Non-hygroscopic. (Do not have an affinity for moisture.)
- Compatible with other ingredients
- Lower molecular weights
- High heat of formation

1.8.3.2 Oxidizer of composite propellant

The composite propellant, by weight, is up to 85 percent composed of oxidizer. In earlier formulations of composite propellants, ammonium nitrate (AN) was used as oxidizer but, as result of further research, AN was replaced with ammonium per chlorate (AP). Ammonium Perchlorate is non-hygroscopic and possesses high solid density of 1.9 g/cm^3. AP, on combustion, produces oxygen to oxidize the fuel matrix along with a release of 193 kJ/mole of heat emery.

$$2NH_4ClO_4 \longrightarrow N_2 + Cl_2 + 4H_2O + 2O_2 + 193\ kJ\ mole^{-1}$$

Powdered aluminum can also be used as fuel in composite propellant since it is only

another fuel to be chemically balanced together with the binder against the oxidizing ability of the ammonium per chlorate [21].

1.9 Types of composite solid propellants

- Plastic Composites
- Rubbery Composites
- Polymer Composites

1.9.1 Plastic composites

Plastic composite propellants are the earlier generation of composite solid propellants in which plastic materials like polystyrene, polyvinylchloride (PVC) or polyisobutene (PIB) are used as binder. PIB is used along with plasticizer such as ethyl oleate or dioctyl sebacate to form a mixture named as plastisol. In case of plastisol used as binder, 90% by weight oxidizer (ammonium per chlorate) is used to form a balanced formulation. Such kind of propellant is much uncomplicated to manufacture and there is no likely risk of exothermic reactions arising within the polymer. Other additives for plastic composites include:

- Aluminum as fuel
- Ammonium picrate as burning rate modifier
- Copper chromate as catalyst to increase burning rate
- Oxamide to produce a slight Platonizing effect
- Lecithin as surfactant ensuring good contact between ingredients

The advantages of plastic composite propellant are as follows:

- It is cheap to produce.
- It can be case bonded.
- Its specific impulse is greater than that of double base propellants.
- It can be aluminized to give high specific impulse of around 2600 ms^{-1}.
- It has good shelf life.

The disadvantages of plastic composite propellants are as follows:

- At lower temperature, its stress resistance is poor as compared to rubbery composite propellant.
- It is not suitable for large motors because of slumping.
- It produces smoky efflux.

On account of above disadvantages, plastic composite propellants are no more

favorable for use and its other alternatives have been developed.

An example of use of plastic composite propellant based missile is Bloodhound missile of United Kingdom [21].

1.9.2 Rubbery composites

In rubbery composite propellants, a hydrocarbon polymer fuel is used as binder with ammonium per chlorate as oxidizer. The binder in such kind of composite propellants requires curing after mixing to develop a cross-linked matrix. Polyurethane (PU) was the first polymer to be used in rubbery composite propellants as fuel matrix. Polyurethane is viscous liquid polyester at room temperature.

During manufacturing, polyurethane is mixed with ammonium per chlorate and additives like aluminum powder and plasticizer. The heating and degassing of this mixture is carried out under vacuum condition. The slurry is then cooled and di isocyanate is added as cross-linking agent. This formulation is cast under vacuum inside motor case. The assembly is kept at higher temperature of about 60^{o} C for few weeks.

1.9.3 Polymer composites

Rubbery composites are now mostly replaced by composite propellants composed of polybutadiene as binder. Polybutadiene is further divided into two sub groups:

- Hydroxyl Terminated Polybutadiene (HTPB)
- Carboxyl Terminated Polybutadiene

The cross linking agent for HTPB is diisocyanate. For CTPB, cross linking agent is epoxides (III) or azidrines (IV).

Poly butadiene acrylic acid acrylonitrile (PBAN) is a carboxyl terminated pre polymer that is cross linked by epoxides or aziridines.

For polymer composites, mixture of oxidizer, fuel and other additives are cast into motor case and cured for few weeks at temperature of about 60^{o}C.

1.9.3.1 *Advantages of polymer composites*

The advantages of HTPB and CTPB propellants are as below:

- They possess brilliant mechanical properties.
- They have excellent case bonding ability.
- They can be aluminized.
- They exhibit smooth burning.

1.9.3.2 Disadvantages of polymer composites

Few of the disadvantages of HTPB and CTPB propellants are:

- To acquire physical properties, careful curing is needed otherwise cracks may arise during storage.
- They produce smoky exhaust during propellant burning and it is due to hydrogen chloride formation that creates large white plume. Smoky exhaust make signature for detection of propellant burning during flight.

1.10 Typical compositions of composite propellants

Table 1. 1 Compositions of some typical composite propellants [21]

Component	PU	PBAN	CTPB	HTPB
Ammonium Perchlorate	70	69	63	70
Matrix polymer	21	11	10	12
Aluminum	8	15	17	18
Di-octyladipate	-	4	-	-
HMX	-	-	10	-
Bonding agent	1	1		-
Specific Impulse (ms^{-1})	2400	2260	2600	2550

Chapter 2

Literature Review

Literature survey was performed in two stages. At first literature was reviewed for the preparation of copper oxide and similar nanoparticles and for their characterization. In second stage, literature related to use of copper oxide and other nanoparticles in composite propellant their effects on thermal decomposition of composite propellant was studied.

2.1 CuO nanoparticles synthesis

2.1.1 By copper chloride and acetic acid

Y. Aparna et al synthesized CuO nanoparticles by sol gel technique in which aqueous $CuCl_2.6H_2O$ was treated with glacial acetic acid. The solution was heated to 100 ^oC with continuous stirring. Hot solution was reacted with sodium hydroxide solution drop wise till the pH of solution became 7. The precipitates were centrifuged and then washed with deionized water. The precipitates were left for drying for one day to get CuO nanoparticles. For thermal analysis, TG-DTA analysis of nanoparticles was performed. The morphology was studied through SEM and TEM. Nanoparticles of spherical shape and with particle size less than 50 nm were observed [23].

2.1.2 By copper nitrate and ethanol

R. Etefagh et al synthesized CuO nanoparticles through sol gel technique by treating a precursor solution of ethanol and water with copper nitrate. Citric acid and ethylene glycol were also added as polymerization and complex agents respectively. The solution was stirred for one hour at 40 ^oC to get a green solution. This solution was maintained under reflux at 100-110 ^oC for 4 hour. In that way, a wet gel was prepared that was calcinated for 1 hour at 600 ^oC & then size reduction was performed by milling to obtain nanoparticles of CuO [24].

L. J. Chen et al synthesized CuO nanoparticles by mixing copper nitrate 3-hydrate with ethanol and sodium hydroxide to form black precipitates. CuO nanocrystals of different surface area were then achieved by annealing at diverse temperatures [25].

2.1.3 By copper sulfate and ammonium chloride

G. Mustafa et al used copper sulfate pentahydrate and mixed it with hydroxyl ammonium chloride and NaOH was then used as stabilizing agent. The characterization of prepared nanoparticles was performed through XRD and SEM analysis. Single phase monoclinic structure was observed by XRD analysis with average crystallite size of 20-28 nm [26].

2.1.4 By copper sulfate and sodium carbonate

E. Darezereshki et al synthesized CuO nanoparticles by reacting Copper (II) Sulfate 5-hydrate with Sodium. It was then thermally decomposed in muffle furnace at 750^{o}C for 2 hours to get final product of CuO nanocrystals. The mean crystallite sizes of prepared CuO nanoparticles was calculated as 70 nm by Debye-Scherer equation. Spherical shaped nanoparticles were observed in SEM images [27].

2.2 Mixing nanoparticles with composite propellant

Many researchers focused their attention on the effect of different types of nanoparticles as catalyst in thermal decomposition of composite propellant and its ingredients especially on ammonium perchlorate (AP).

2.2.1 Mixing of CuO nanoparticles in AP

Ayoman et al prepared spherical shaped CuO nanoparticles by physically grinding the procured micro particles of CuO using the planetary ball mill method. The characterization was done by XRD and SEM. Nanoparticles of 82 nm average size were prepared by this method. The prepared nanoparticles were mixed with AP in different proportions and thermal effects were studied by TGA and DSC technique [28].

2.2.2 Mixing of bimetallic nanocrystals with AP

Pratibha et al prepared nanocrystals using by using double metals such as Copper and Cobalt, Copper and Iron, Copper and Zinc etc. The bimetals were prepared by using of hydrazine and ethylene glycol. Nanocrystals smaller than 40 nm were synthesized by this method. They were employed as catalyst in thermal decomposition examination of ammonium perchlorate and proved effective [29].

2.2.3 Mixing of magnesium oxide nanoparticles with composite propellant

Zaheer-ud-din et al used magnesium oxide (MgO) nano particles to catalyze the composite propellant material based on HTPB and AP. X-ray diffraction (XRD)

technique and scanning electron microscope (SEM) were used to characterize the MgO nano particles before they were added to the propellant material. The average size of the particles was found to be approximately 20-30 nm. The decomposition peak temperature of the propellant decreased nearly 22^{o}C due to the addition of two percent of MgO as a catalyst [30].

Chapter 3

Experimental Techniques and Methods

Theory of experimental techniques and method involved in the synthesis of CuO nanoparticles and their characterization is included in this chapter. Theoretical detail of thermogravimetic analysis is also given this chapter.

3.1 Preparation of CuO nanoparticles

For the preparation of CuO nanoparticles, aqueous precipitation followed by thermal decomposition of precipitates in furnace was employed. Solution of copper sulfate and sodium carbonate were reacted under constant stirring and heating to form black green precipitates. The precipitates were washed and dried. The thermal decomposition of of green precipitates in muffle furnace under elevated temperature produced black colored nanoparticles of CuO. The experimental procedure for preparation of CuO nanoparticles is discussed in detail in chapter 4 of this thesis report.

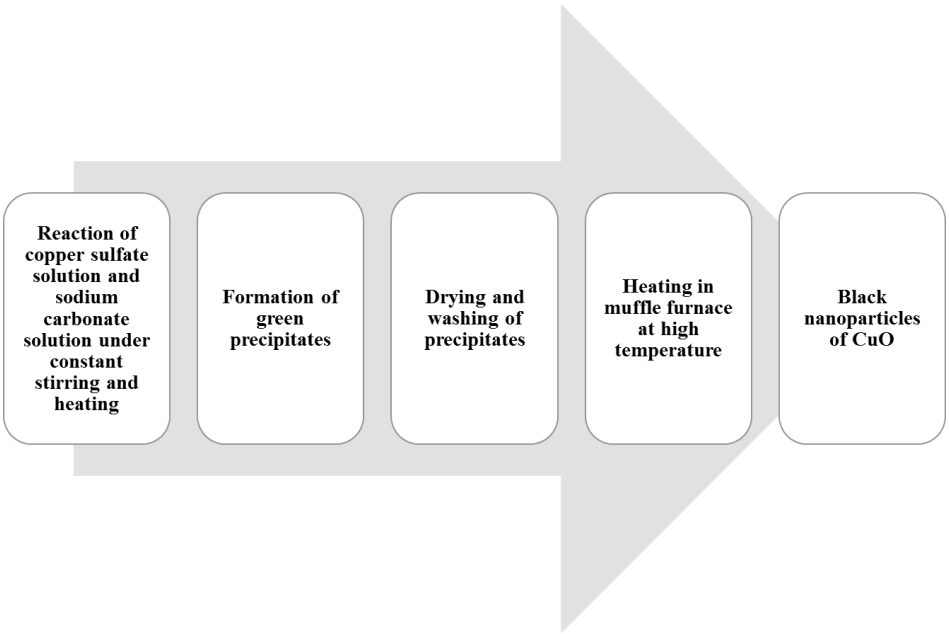

Figure 3. 1 Block diagram for CuO nanoparticles preparation

3.2 Techniques for characterization of nanoparticles

Following characterization techniques were employed in this research work for the characterization of CuO nanoparticles

3.2.1 Fourier Transform Infrared (FTIR) Spectroscopy

In FTIR spectroscopy, an infrared spectra is taken by bringing together an interferogram of a sample signal through interferometer. Fourier transform is then performed to get the spectrum.

Before explaining the working principle of FTIR spectrometer, following definitions are necessary to learn:

- The investigation for the interaction of light with matter is called spectroscopy and if light used is infrared light, then this type of spectroscopy is known as Infrared spectroscopy.
- Spectrum is actually a plot of light intensity against its wavelength or wavenumber.
- Infrared spectrum is measured by Infrared Spectrometer [31].

Information regarding the type of molecule present in sample and its concentration is presented by analysis of infrared spectra.

3.2.1.1 Infrared spectrum

In infrared spectrum, x-axis is plotted in descending order i.e., higher wavenumber on left side of plot. For example in Figure 3.2, 4000 cm^{-1} is on left of plot whereas 500 cm^{-1} is on right.

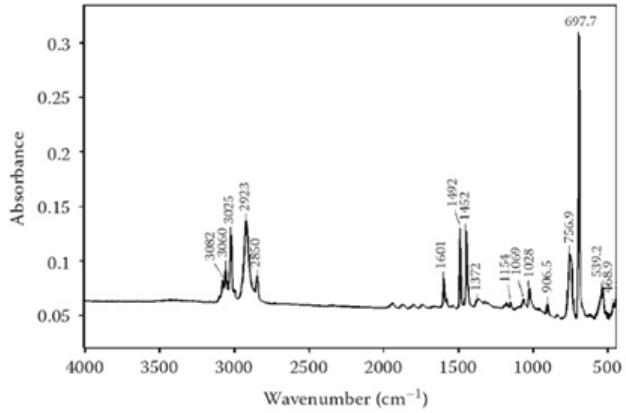

Figure 3.2 Infrared spectrum plotted as absorbance

This convention is followed in all plots of FTIR spectra. Y-axis is plotted in absorbance units. Absorbance is the quantity of light absorbed by a sample.

In percent transmittance spectrum, peaks are pointed down as shown in Figure 3.3.

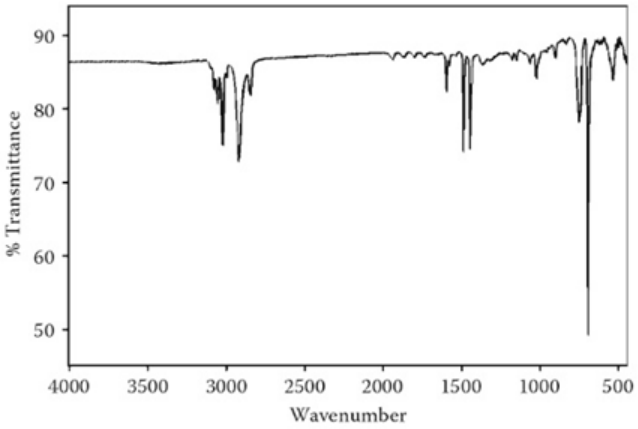

Figure 3.3 The infrared spectra plotted in % Transmittance

3.2.1.2 Principle of FTIR spectrophotometry

The absorption of light by the molecule depends on the bonds present in it. Infrared radiation is passed throughout a sample in this technique. The sample absorbs few of the infrared radiation and a part of it passes through the sample. Such infrared spectrum of some sample is used as its fingerprint. Two different compounds cannot give the exact same infrared spectrum due to the unique combination of atoms in different compounds or materials. The amount of material present in a sample can also be judged by the size of the peaks in the spectrum. Infrared Spectroscopy along with modern software algorithm is therefore a valuable tool for quantitative analysis.

3.2.1.3 Sample analysis process

The sample analysis process is carried out as following steps:

Source

The source consists of glowing black body that releases infrared energy beam. The amount of energy that falls on the sample is controlled by passing infrared beam through an aperture.

Interferometer

Interferometer performs spectral encoding of the beam.

Sample

On striking the sample, a part of beam is absorbed and remaining is transmitted or reflected.

Detector

The beam is lastly passed through a detector for the investigation.

Computer

From computer software, user obtains the final infrared spectrum for further interpretation and manipulation.

Percent transmittance is calculated by comparing the final infrared spectrum with background spectrum. Background spectrum is obtained without sample in the path of beam. This method reduces the chances of error in spectral features.

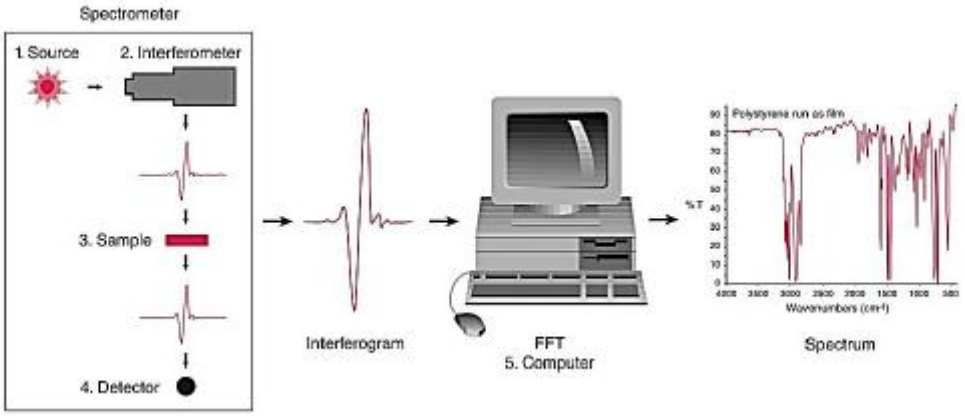

Figure 3.4 Instrumentation and data processing in FTIR

3.2.2 X-Ray diffraction (XRD)

XRD has been a very supportive characterization practice for non-destructive study of diverse properties of materials. For instance, crystallographic structure and chemical composition of materials can be verified by XRD analysis. XRD technique is also useful in determining thickness of thin films. X-ray diffractogram offers excellent information about phase composition, crystallite size, lattice strain and crystallographic orientation.

3.2.2.1 Fundamental principle

The theoretical principle of XRD can be explained by Figure 3.5 in which diffraction angle 2θ is the angle between the incident and diffracted X-rays.

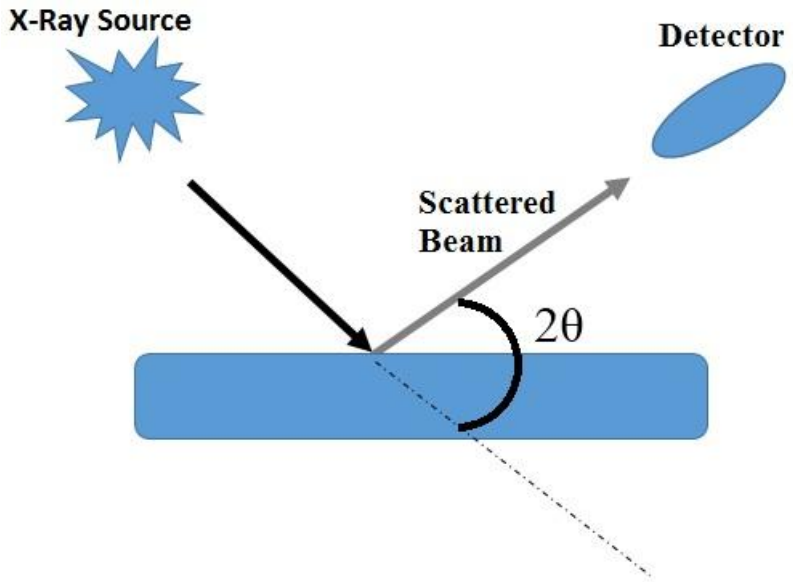

Figure 3.5 XRD Principle

A plot between reflected intensities and the detected angle 2θ is generally referred to as diffraction spectrum. The proper selection of correct anode and energy of accelerated electrons result in X-rays with specified wavelength and energy. X-rays with single wavelength or monochromatic radiations are employed for improved experimental consequences.

3.2.2.2 Bragg's Law

Bragg's law is expressed as equation below:

$2d \sin\theta = n\lambda$

Where

λ = wavelength

d = spacing between atomic planes

θ = angle of diffraction.

A simple crystal with lattice planes separated by distance d is shown in Figure 3.5. The angle between incident radiation and diffracting plane is given as angle θ in Bragg's law. In case of first order diffraction, n is taken as 1 and with known values of θ and λ, inter-planar spacing or value of d for a particular plane can be calculated. In idealized diffraction pattern, indexing of peaks can be achieved by assigning correct Miller indices to all the peaks.

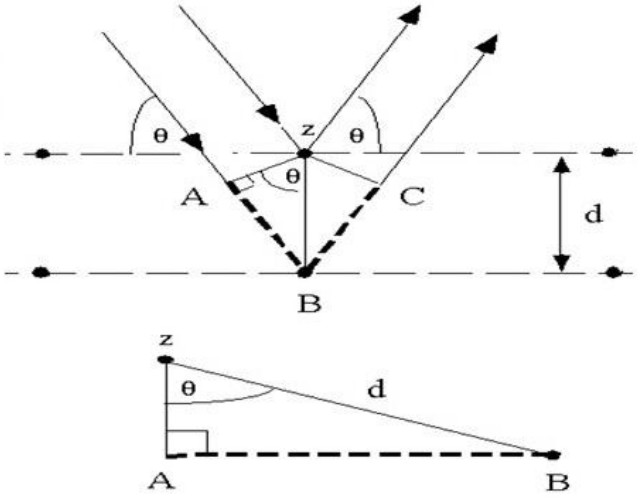

Figure 3.6 Bragg's Law

3.2.2.3 Calculation of crystallite size

An equation by Debye Scherer can be employed to calculate dimensions of particles as following:

$$D_{av} = \frac{57.3K\lambda}{\beta \cos\theta}(nm)$$

D is thickness of particle, β is the line broadening at half the maximum intensity, K is a factor associated to crystal type or shape and λ is the wavelength of the incident X–ray beam [32].

3.2.3 Scanning electron microscopy (SEM)

SEM has been employed in investigation of structure of matter and estimations of its dimensions over a wide range of magnification. In this instrument, radiations with shorter wavelengths are employed to study better-quality structural specifics of materials. An electron beam is used for this purpose. The incidence of electron beam on sample provides detailed study of information about crystal structure and orientation. The details received from the interaction of beam and sample is produced in the form of image.

Figure 3.7 Scanning Electron Microscope

3.2.3.1 Working principle of SEM

Electrons produced in electron gun in the form of beam are applied on the surface of sample. The atoms on the surface of sample release electrons as a result of bombardment of electron beam from electron gun. Due to vacant place in electronic shell of atom, an electron from a shell with greater energy seals the empty place. Due to difference in energy level of two electrons interaction, an x-ray is produced. In this way secondary electrons and high energy backscattered electrons are formed. The intensity of emission of electrons is the structural feature of the specimen. The emitted electrons gives the details about the specimen. The intensity of electrons varies the resulting signal strength and fluorescent image is produced in cathode ray tube. [33]

3.2.3.3 Sample preparation

The nature of the sample defines the requirement of sample preparation for SEM analysis. If the sample is electrical insulator, then a coating of conductor layer is applied on its surface. The materials used for surface coating are usually carbon and gold. The choice of conducting material depends on the required data by SEM analysis. In case of elemental analysis, carbon coating is applied as preference. If the

instrument can perform under vacuum conditions then the requirement of conductive coating may be relaxed.

3.3 Thermal Analysis

In thermal analysis all the changes in properties of material or substance are considered that occur due to change in temperature [34]. Hence, the term thermal analysis applies to many experimental techniques that are shown in Figure 3.8 below:

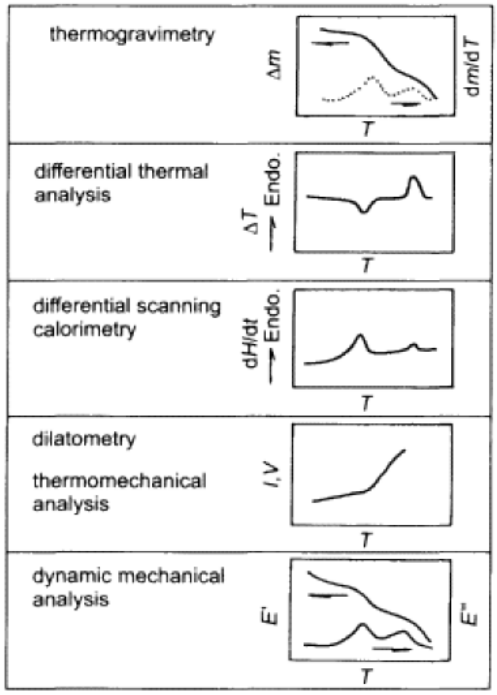

Figure 3. 8 Representative thermal analysis curves [34]

Thermal analysis techniques are valuable for many scientific and industrial purposes due to their capability to distinguish materials over a wide range of temperatures. A thermal analysis apparatus as shown in Figure 3.9 consists of furnace in which temperature and atmosphere is controlled. For the monitoring of physical properties such as temperature and humidity, sensors are installed. A temperature programmer is installed to set the temperature program according to the requirement. The changes during the process are recorded and can be plotted to observe the trend.

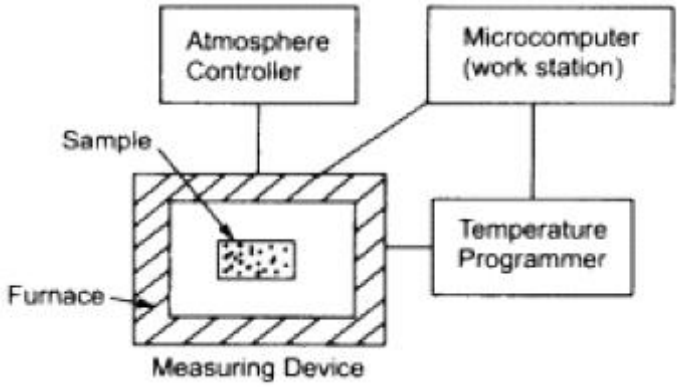

Figure 3. 9 Block diagram of thermal analysis instrument

3.3.1 Thermogravimetry

In thermogravimetry, variation in the mass of sample by changing temperature is studied. Few of the properties that can be characterized by thermogravimetry technique are listed below:

- Sublimation
- Vaporization
- Oxidation
- Reduction

Kinetics of the physicochemical progressions happening in the sample can also be studied by using thermogravimetry data. Precautionary steps are required to establish optimum conditions for thermogravimetry analysis.

3.3.1.1 Thermogravimetry curves

In Figure 2.12, thermogravimetry curve of a single stage reaction is shown.

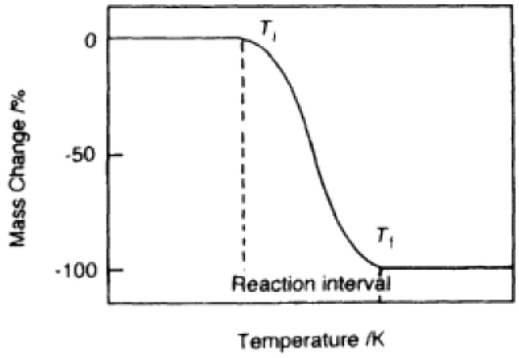

Figure 3. 10 Thermogravimetry curve

Two temperatures are shown on curve as T_i and T_f. T_i initial or procedural temperature at which the reaction begins whereas T_f is final temperature after decomposition. Both T_i and T_f and the reaction interval (T_i - T_f) depend on the experimental conditions.

3.3.1.2 Thermo balance

Thermo balance is used for the recording of thermogravimetry curves. Thermo balance consists of following parts:

- Sample holder
- Electronic microbalance
- Furnace
- Temperature Programmer
- Computer
- Or Chart Recorder

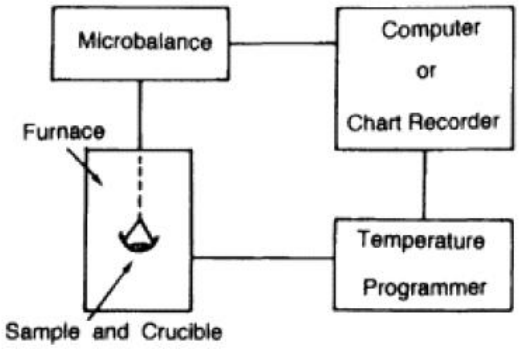

Figure 3. 11 Thermo balance

3.3.2 Derivative thermogravimetry (DTG)

An example of DTG is shown as Figure 3.12. At time of no change in mass the DTG curve remains as minimum.

The height of peak at any stage exhibits that the change in mass is higher at that specific temperature. This change is due to the chemical reactions occurring within the substance by the change in temperature.

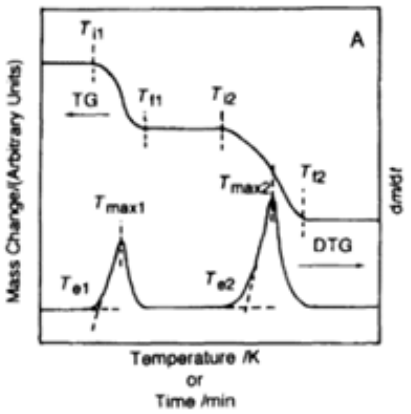

Figure 3. 12 Two-stage TG curve and the corresponding DTG curve

3.3.3 Differential thermal analysis (DTA)

In DTA technique, an inert reference and test sample are heated and cooled under same conditions and change in temperature is documented. Differential temperature is plotted versus time or temperature. The variation in sample is estimated by absorption or evolution of heat comparative to the inert reference.

3.3.3.1 Construction and working of DTA

In Figure 3.13 a classical differential thermal analyzer is shown. It consists of a sample holder assembly that is positioned in the mid of the furnace. Sample is placed in one holder and reference inert material such as α-alumina is filled in the other holder. The used reference material must be thermally inert substance that remains in the same phase over operational range of the experiment. Thermocouples are employed to measure temperature difference between sample and reference. These thermocouples are inserted in each holder. A temperature programmer controls the temperature of the furnace. [35]

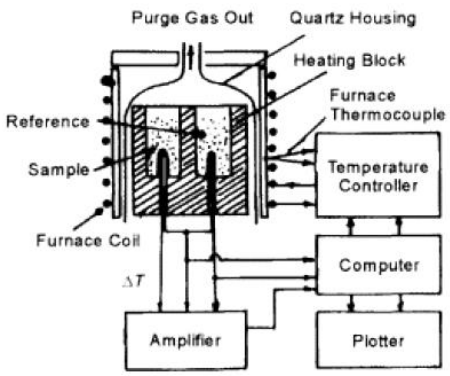

Figure 3. 13 Schematic of differential thermal analyzer

3.3.3.2 DTA curve

Temperature difference is plotted against temperature or time in DTA curve. The slope of the DTA curve changes due to phase transition as shown in Figure 2.16.

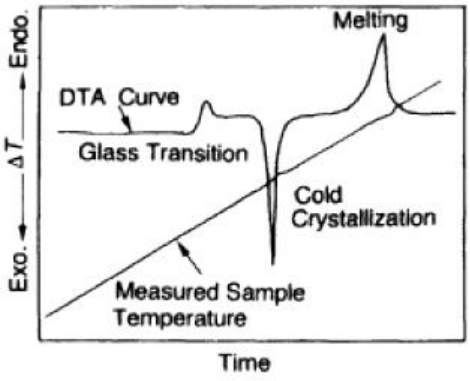

Figure 3.14 DTA curve

The temperature of the sample holder increases above the programmed value due to evolution of heat during crystallization. On the contrary, the temperature of the sample holder decreases during melting due to absorption of heat. In this way, the real temperature of the sample varies during the experiment.

The temperature calibration is done by employing some standard reference material whose phase transition temperatures are known and in the similar transition temperature range as that of the sample to be examined.

3.3.4 Simultaneous thermal analysis

Simultaneous thermal analysis is performed on facility offered by many thermal analyzer manufacturers. Due to similar experimental conditions, better and speedy comparative data can be achieved by using simultaneous analyzer. For example, in evolved gas analysis, the gaseous products evolved during a TG measurement are readily analyzed by attaching a suitable instrument to the TG apparatus.

A same heating program is designated to the sample. Atmosphere, gas flow rate and sample crucible also remain alike. A third curve of DTG is also possible to construct that forms this arrangement as more helpful tool for analysis.

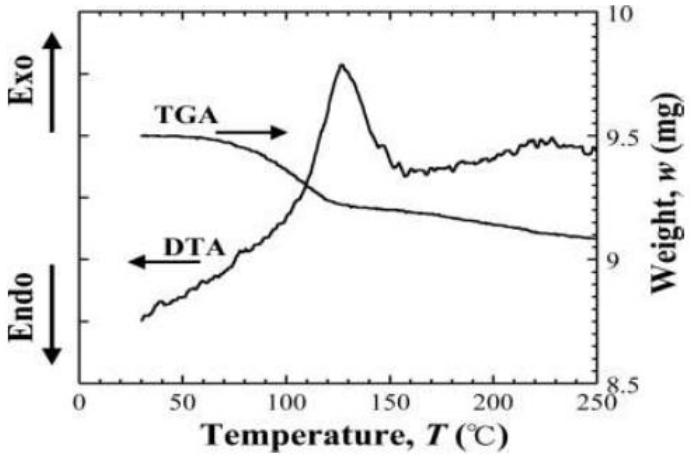

Figure 3. 15 TG/DTA curve

Chapter 4

Experimental Setup

Experimental setup and methods actually used for synthesis of CuO nanoparticles, their characterization and apparatus used for thermal analysis are presented in this chapter.

4.1 Synthesis of CuO nanoparticles

4.1.1 Chemicals used

Table 4. 1 List of chemicals

Chemical	Formula	Grade	Manufacturer	CAS No.
Copper (II) sulfate pentahydrate	$CuSO_4.5H_2O$	AR	Honeywell	7783-20-2
sodium carbonate	Na_2CO_3	AR	Merck	497-19-8

4.1.2 Apparatus

- Weighing balance
- Heating mantle
- 1000 ml glass beaker
- Overhead stirrer
- Heating oven
- Muffle furnace
- Filter paper
- Funnel

4.1.3 Preparation of reagents

- 300 ml of 0.5 molar copper (II) sulfate pentahydrate ($CuSO_4.5H_2O$) solution was made by 37.431 g $CuSO_4.5H_2O$ in 300 ml deionized water.
- 300 ml of 0.5 molar sodium carbonate (Na_2CO_3) solution was made by 15.9 g Na_2CO_3 in 300 ml of deionized water.

4.1.4 Procedure

- 300 ml of 0.5 molar copper (II) sulfate pentahydrate ($CuSO_4.5H_2O$) solution was added in 300 ml of 0.5 molar sodium carbonate (Na_2CO_3)

solution with vigorous stirring by overhead stirrer and maintaining temperature of 80 ^{o}C for one hour to get precursor as green precipitates of the basic copper sulphates [brochantite $Cu_4 (SO_4) (OH)_6$ and posnjakite $Cu_4 (SO_4) (OH)_{6.H2O}$] precipitate.

- The precipitates were separated by filtration and filtered precipitates were washed with warm deionized water for removing any possible remaining ions in final product.
- The washed precipitates were dried at 70˚C in air for two hours in an oven.
- The final product as CuO nano crystals was achieved by thermal heating of green precipitates in a muffle furnace at 750^{o}C for two hours.
- The steps involved in experimental procedure is shown in figure 4.1

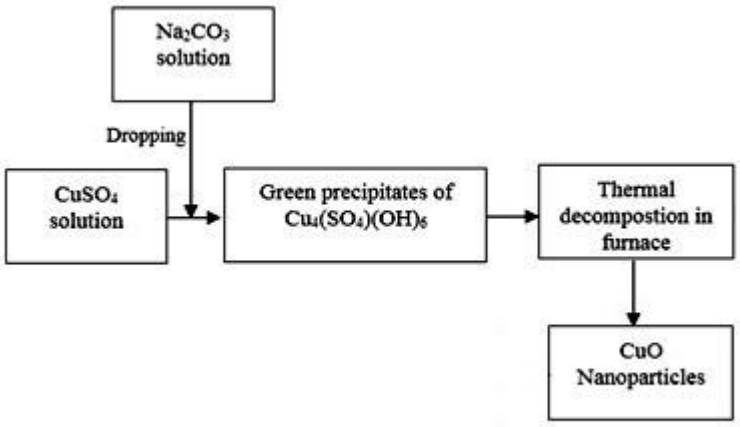

Figure 4. 1 Experimental procedure

- Chemical reactions are shown as equations below:

$$Cu_4(SO_4)(OH)_6.xH_2O \xrightarrow{80-170^{\circ}C} CuSO_4.3Cu(OH)_2 + xH_2O \quad (1)$$

$$CuSO_4.3Cu(OH)_2 \xrightarrow{250-400^{\circ}C} CuSO_4.2Cu(OH)_2 + CuO + H_2O \quad (2)$$

$$CuSO_4.2Cu(OH)_2 \xrightarrow{610-700^{\circ}C} 3CuO + 2H_2O + SO_2 + \frac{1}{2}O_2 \quad (3)$$

- Intermediate green precipitates and final black CuO nanoparticles were as shown in figure 4.2 below.

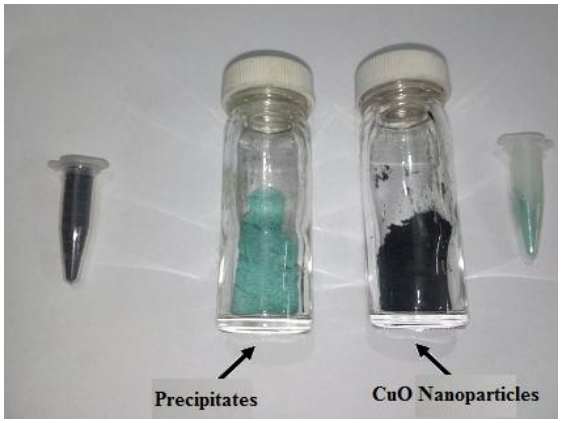

Figure 4. 2 Green precipitates and black CuO nanoparticles

4.2 Characterization of CuO nanoparticles

4.2.1 FTIR analysis

FTIR spectroscopy of intermediate green precipitates and final black CuO nanoparticles were performed by using Perkin Elmer Spectrum Two FTIR. The instrument is shown in Figure 4.3.

Figure 4. 3 Perkin Elmer spectrum two FTIR

The instrument was attached with computer with comprehensive FTIR software of Spectrum 10 to facilitate data collection, processing and results generation. The interface is shown in Figure 4.4 below:

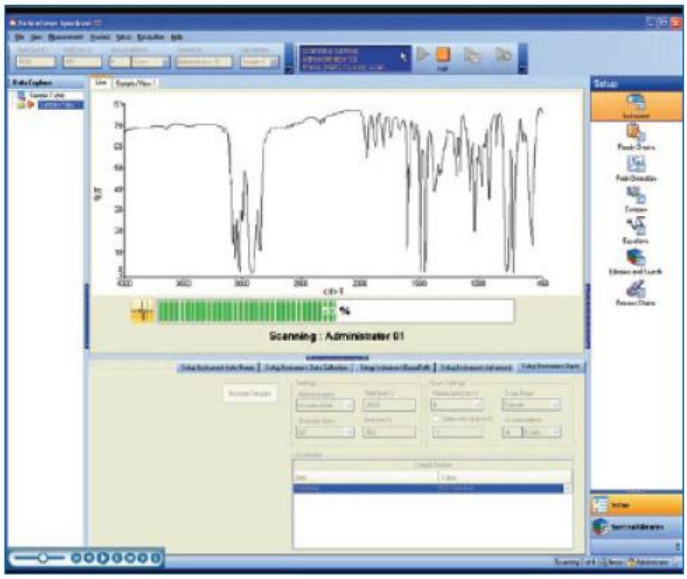

Figure 4. 4 Spectrum 10™ software interface

4.2.2 XRD analysis

PANalytical X'PERT High Score's diffractometer was used for XRD analysis. The diffractometer operated in assistance with International Center for Diffraction Data search and match program. It was used for identification of crystalline mineral phases, although clay minerals could also be characterized by utilizing pre-analysis treatments. Short-wavelength x-rays diffracted off of the regular 3D structures of atoms in crystals; providing signature diffraction patterns. These diffraction patterns were interpreted by using ICDD (International Centre of Diffraction Data) database of characteristic mineral patterns.

4.2.3 SEM Analysis

SEM analysis of CuO nanoparticles was performed by scanning electron microscope (Model: JSM-6490A, Make: JEOL, Japan) as shown in Figure 4.5.

Figure 4. 5 SEM (JSM-6490A)

For specimen treatment, an auto quick coater (Model: JFC=1500, Make: JEOL, Japan) was used as ion sputtering device for 250A^{o} Gold coating. Auto quick coater is shown in Figure 4.7:

Figure 4. 6 JEOL auto quick coater

4.3 Samples preparation for thermal analysis

For the investigation of catalytic effect of CuO nanoparticles on the thermal decomposition of composite propellants, samples were prepared by mixing with

composite propellant. The used composite propellant was composed essentially of AP as oxidizer and HTPB as binder. The samples were made by mixing CuO nanoparticles in different percentages as listed below:

- 100% Composite Propellant
- Composite Propellant with 1% CuO Nanoparticles
- Composite Propellant with 2% CuO Nanoparticles
- Composite Propellant with 3% CuO Nanoparticles
-

4.4 Thermal Analysis

The thermal analysis of samples was performed with diamond TG/DTG instrument as shown in figure 4.8.

Figure 4. 7 Diamond TG/DTG instrument

The instrument was attached to a computer with pyris software for controlling the operation of thermal analyzer. The operational limit of the instrument was from ambient to 1500 ^{o}C. The specifications of TG/DTG instrument are presented in Table 4.2 below:

Table 4. 2 Specifications of TG/DTG instrument

Model No.	Pyris Diamond Series TG/DTA
Make	Perkin Elmer, USA
Temperature range	Ambient to 1500°C
Analysis atmosphere	Air, Ar and N2
Required physical state of samples	liquid and solid

Chapter 5

Results and Discussions

Results obtained by characterization of CuO nanoparticles through FTIR, XRD and SEM are given and explained. The thermal analysis of different samples of composite propellant mixed with CuO nanoparticles are also provided and discussed.

5.1 CuO nanoparticles characterization by FTIR

Figure 5.1 represents the FTIR spectrum recorded for the CuO nanoparticles in the range of 400 to 4,000 cm^{-1}.

- Peaks at 529.81 cm^{-1} and 585.92 cm^{-1} were due to the presence of CuO in final product [36].
- The peaks at 1636.61 cm^{-1} and 3423.26 cm^{-1} were due to presence of moisture in sample [37].

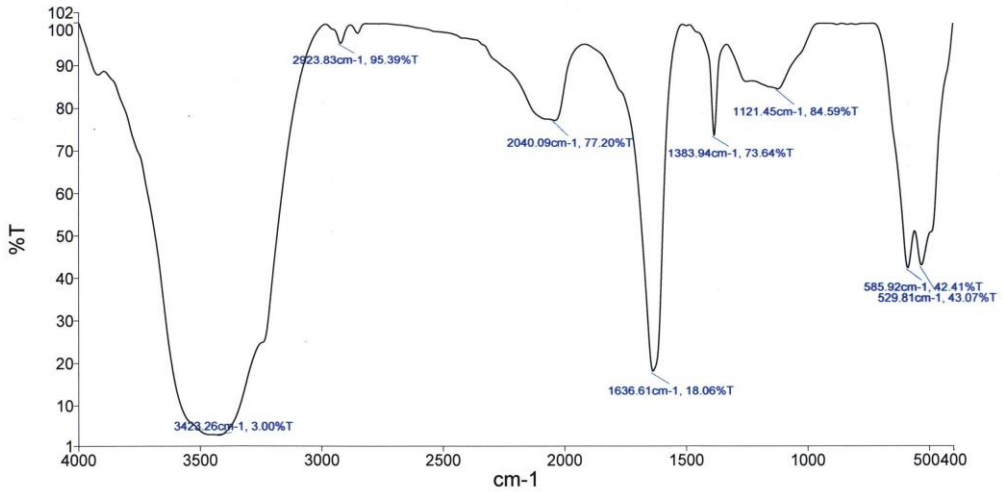

Figure 5. 1 FTIR spectrum of CuO nanoparticles

5.2 Characterization of CuO nanoparticles by XRD

The X-ray diffraction (XRD) was carried out to analyze the phase and to estimate the crystallite size of the samples using X-ray diffractometer (PANalytical X'PERT High Score) with 1.54178 Å Cu-Kα radiation source in the 2θ range from 10˚ to 80˚ (40 KV, 30 mA, step size 0.020, scan rate 0.40 min^{-1}) at room temperature. The XRD patterns with diffraction intensity versus 2θ were recorded.

The results proved that the sample contains Ternoite, syn CuO-Monoclinic and were matched with ICDD File # 05-0661. X-ray diffraction pattern of copper oxide nanoparticles is presented in figure 5.2.

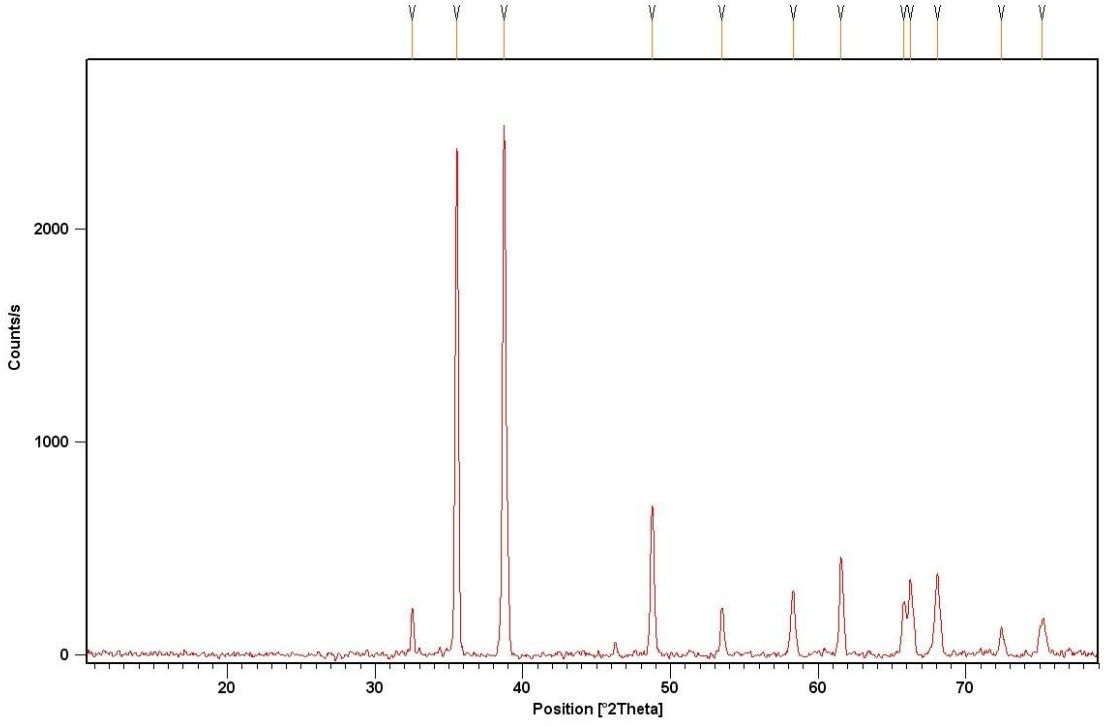

Figure 5. 2 XRD analysis of CuO nanoparticles

XRD observations data is presented in Table 5.1. Average crystallite size was also calculated by using Debye-Scherer equation.

$$D = \frac{0.9\lambda}{\beta Cos\theta}$$

Where

λ (for Cu Kα average) = 1.54178 Å = 0.154178 nm

β = Full width at half maximum of XRD peak in radian

θ = XRD peak position

Table 5. 1 XRD observations and calculations

No.	Pos. [°2Th.]	d-spacing [Å]	FWHM [°2Th.]	Rel. Int. [%]	Dp (nm)	Dp Average (nm)
1	32.5241	2.75304	0.1574	9.27	54.95	62.39
2	35.5469	2.52556	0.0984	96.64	88.62	
3	38.7126	2.32601	0.1771	100	49.70	
4	48.7318	1.86866	0.0984	27.6	92.64	
5	53.4764	1.71352	0.1574	9.37	59.07	
6	58.2957	1.58282	0.2362	12.73	40.25	
7	61.5328	1.50709	0.0984	19.04	98.21	
8	65.8013	1.41929	0.2362	10.79	41.87	
9	66.2446	1.41087	0.1181	14.97	83.95	
10	68.0851	1.37714	0.1181	16.19	84.85	
11	72.4252	1.30494	0.3149	5.5	32.68	
12	75.1593	1.26307	0.48	6.52	21.83	

Hence, average crystallite size of CuO nanoparticles calculated by Debye-Scherer equation was 62.39 nm.

5.3 Characterization of CuO nanoparticles by SEM

The surface morphology of the sample was obtained using scanning electron microscopy (JEOL, JSM-6490A, Japan).

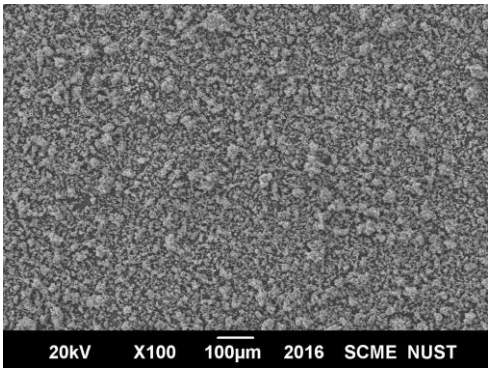

Figure 5.3(a)

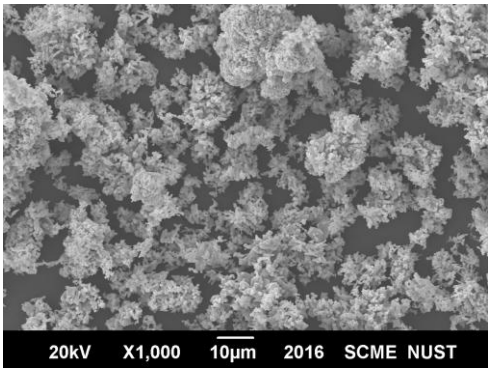

Figure5.3(b)

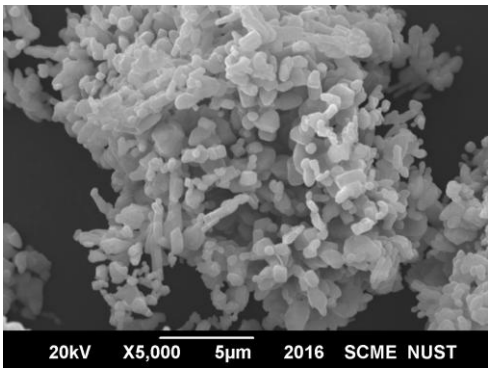

Figure 5.3(c)

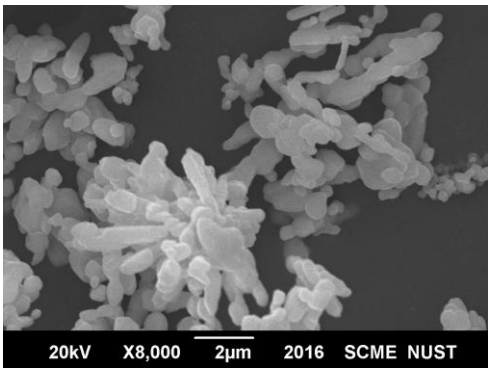

Figure 5.3(d)

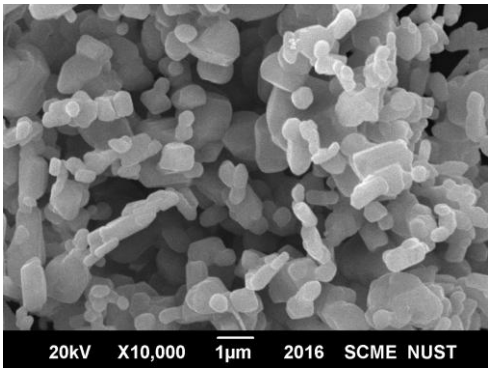

Figure 5.3(e)

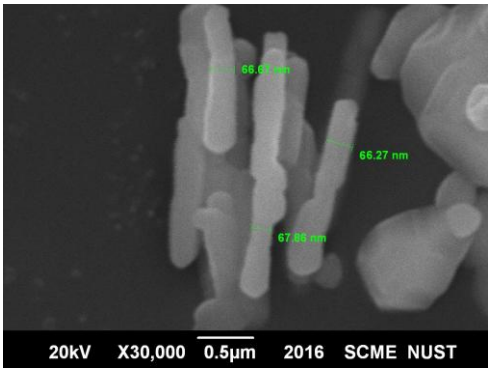

Figure 5.3(f)

Figure 5. 3 (a, b, c, d, e and f) SEM images of CuO nanoparticles

Figure 5.3 (a, b, c, d, e and f) represents the SEM images of CuO nanoparticles obtained at magnifications of x100, x1000, x5000, x8000, x10000 and x30000.

From the SEM images of CuO nanoparticles, it was observed that the particles are well-dispersed cylindrical shape, accompanying almost well-defined and uniform crystalline structure. There was also a higher tendency of agglomerations. In some regions, the big nanoparticles were surrounded by smaller nanoparticles. The average diameter of rod shaped nanoparticles was found to be 66.93 nm.

5.4 TGA and DTG of composite propellant samples

5.4.1 Comparison of TG curves

Thermogravimetry analysis of composite propellant without CuO nanoparticles and composite propellant mixed with CuO nanoparticles in different percentages is presented in Figure 5.4 below:

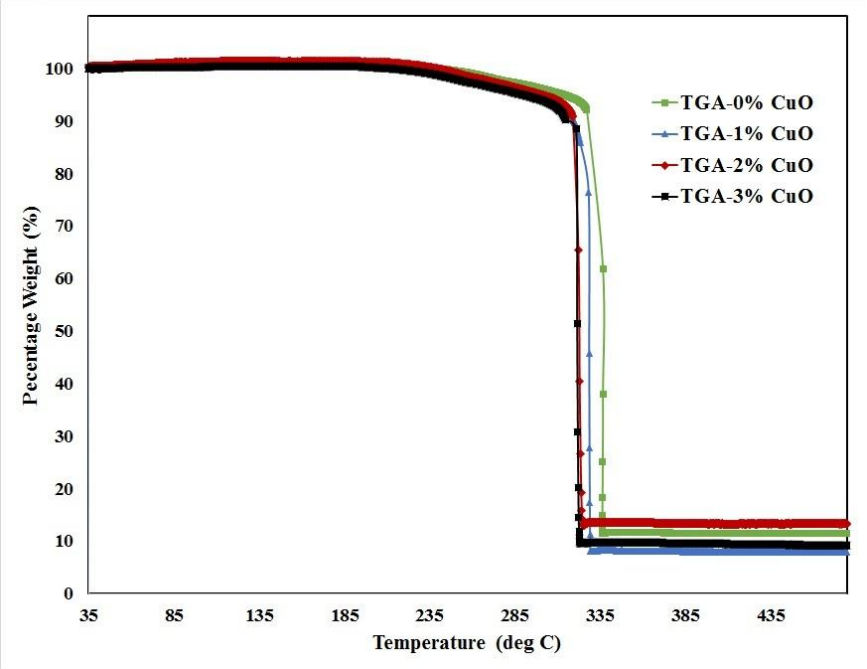

Figure 5. 4 TGA curves

TGA curves show that the weight loss pattern for different samples is quite similar

and there is no significant change. The decomposition of the samples starts near 250^{o}C. Relatively slow initially but beyond the temperature of 320 ^{o}C, it becomes quite rapid.

5.4.2 Comparison of DTG curves

Differential thermogravimetry curves of the samples are shown as figure 5.5. By comparing the curves, it was evident that the peak decomposition temperature of composite propellant was decreased by increasing CuO nanoparticles percentage in samples. For pure composite propellant sample, the peak decomposition temperature was around 336 ^{o}C. But by mixing CuO nanoparticles in composite propellant, the peak decomposition temperatures were decreased to 328°C, 322°C and 321^{o}C with 1%, 2% and 3% CuO nanoparticles in composite propellant samples.

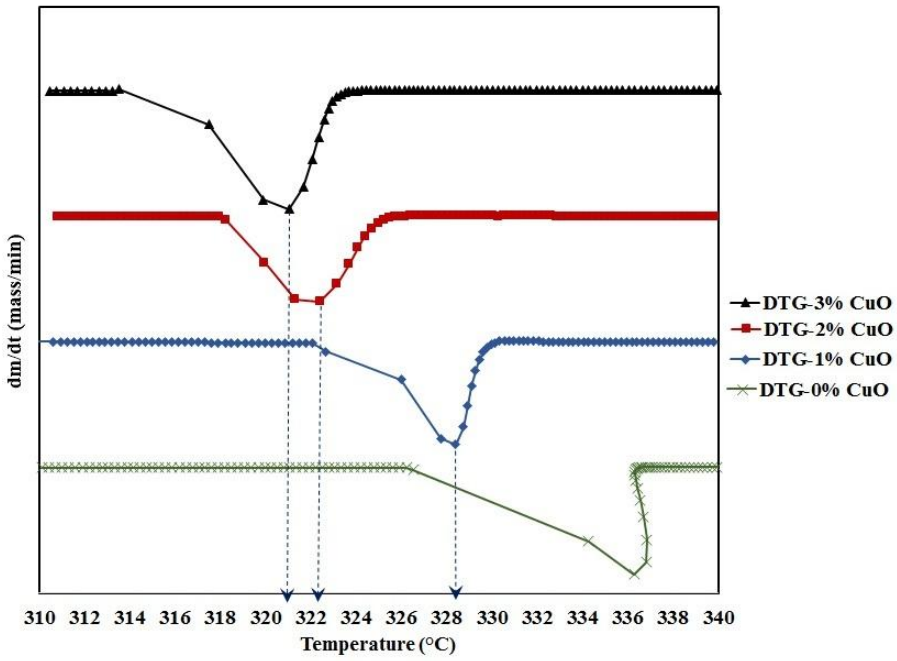

Figure 5. 5 DTG curves

Chapter 6

Conclusions

Synthesis of CuO nanoparticles and its characterization by FTIR, XRD and SEM has been performed in this work. Study of catalytic effect of CuO nanoparticles on decomposition of composite propellant has also been carried out by using TG and DTA analysis technique.

6.1 Synthesis of CuO nanoparticles

It has been found that synthesis of CuO nanoparticles can be done by aqueous precipitation method using solution of Copper (II) Sulfate Pentahydrate ($CuSO_4.5H_2O$) and sodium carbonate ($CaCO_3$) to produce green precipitates. The filtration, washing, drying of precipitates and its thermal decomposition at 750^oC in muffle furnace produces black nanoparticles of CuO. The used chemicals are easily available in market and this synthesis method is easy to carry out in laboratories with usual apparatus.

6.2 Characterization of CuO nanoparticles

Composition of CuO nanoparticles has been investigated by using FTIR analysis and found essentially composed of CuO. The XRD analysis results show that the sample contains Ternoite, syn-CuO-Monoclinic and matched with ICDD File # 05-0661. SEM analysis of CuO nanoparticles gives results as thin nano rods and these small rods are of almost equal dia. The average diameter of nano rods is 66.93 nm.

6.3 Thermal analysis of composite propellant

Composite propellant made up essentially of AP and HTPB has been used. The prepared copper oxide nanoparticles has been mixed in different proportions as 1%, 2% and 3% with composite propellant to study the catalytic effect of mixed CuO nanoparticles. The results of analysis have shown a decreasing trend in decomposition temperature of composite propellant by increasing the percentage of CuO nanoparticles. The peak decomposition temperatures have been found as Reduction in thermal decomposition temperature from 336^oC to 321^oC was observed by adding 3% copper oxide nanoparticles in composite propellants.

6.4 Recommendations for future work

Kinetic study of thermal decomposition of composite propellant mixed with CuO nanoparticles may also be performed.

References

[1] K. Kalantar-zadeh and B. Fry, Nanotechnology-Enabled Sensors, New York: Springer, 2008, pp. 1-12.

[2] C. d. M. Donega, "The Nanosciences Paradigm: "Size Matters!"," in Nanoparticles: Workhorses of Nanosciences, New York, Springer, 2014, pp. 1- 12.

[3] N. Kumar and S. Kumbhat, Essentials in Nanoscience and Nanotechnology, New Jersey: Wiley, 2016.

[4] A. Rasheed and F. A. Khalid, "Fabrication and properties of CNTs reinforced polymeric matrix nanocomposites for sports applications," in International Symposium on Advanced Materials, 2014.

[5] R. J. Martín-Palma, M. Manso and V. Torres-Costa, "Optical Biosensors Based on Semiconductor Nanostructures," Sensors, vol. 9, pp 5149-5172, 2009.

[6] H. Presting and U. Konig, "Future nanotechnology developments for automotive applications," Materials Science and Engineering, vol. 23, pp. 737-741, 2003.

[7] J. Pannu, "In Vitro Antibacterial Activity of NB-003 against Propionibacterium acnes,"Antimicrobial Agents and Chemotherapy, vol. 55, no. 9, p. 4211–4217, 2011.

[8] C. Rigo, "Active Silver Nanoparticles for Wound Healing," International Journal of Molecular Science, vol. 14, pp. 4817-4840, 2013.

[9] Syduzzaman, "Smart Textiles and Nano-Technology: A General Overview," Textile Science & Engineering, vol. 5, no. 1, 2015.

[10] T. Faunce, "Exploring the safety of nanoparticles in Australian sunscreens," Int. J. Biomedical Nanoscience and Nanotechnology, vol. 1, no. 1, pp. 87-94, 2010.

[11] C. Matteo, "Current and Future Nanotech Applications in the Oil Industry," American Journal of Applied Sciences, vol. 9, no. 6, pp. 784-793, 2012.

[12] F. Tingming, "Preparation of CuO Modified SBA-15 and Applications as Catalyst in AP/HTPB Solid State Propellants," Combustion Science and Technology, vol. 181, no. 6, 2009.

[13] W. Kang, C. Zhao and Q. Shen, "Lithium Storage Capability of Nanocrystalline CuO Improved by its Water-Based Interactions with Sodium Alginate," Int. J. Electrochem. Sci., vol. 7, no. 1, pp. 8194 - 8204, 2012.

[14] N. M. Deraz and M. Fouda, "Fabrication and Magnetic Properties of Cobalt-Copper Nano- Composite," Int. J. Electrochem. Sci., vol. 8, no. 1, pp. 2682 - 2690, 2013.

[15] A. Rahnama and M. Gharagozlou, "Preparation and properties of semiconductor CuO," Opt Quant Electron, vol. 44, no. 1, p. 313–322, 2012.

[16] K. Nemade and S. Waghuley, "Optical and Gas Sensing Properties of Cuo Nanoparticles Grown by Spray Pyrolysis of Cupric Nitrate Solution," International Journal of Materials Science and Engineering, vol. 2, no. 1, pp. 63-66, 2014.

[17] H. Kidowaki, "Fabrication and Characterization of CuO-based Solar Cells," Journal of Materials Science Research, vol. 1, no. 1, pp. 138-143, 2012.

[18] Y. Zeraatkish, M. Jafarian and M. Mahjani, "Fabrication and Electrochemical Behavior of Monoclinic CuO and CuO/Graphite Composite Nanoparticles as Cathode in an Alkaline Zn-CuO Battery," J. Nano Struct., vol. 5, no. 3, pp. 251-256, 2015.

[19] M. Baghbanzadeh, D. Rana, T. Matsuura and Q. Lan, "Effects of hydrophilic CuO nanoparticles on properties and performance of PVDF VMD membranes,"Desalination, vol. 369, pp. 75-84, 2015.

[20] A. H. Salama, "Effect of magnetic and nonmagnetic nano metal oxides doping on the critical temperature of a YBCO superconductor," Adv. Nat. Sci: Nanosci. Nanotechnol., vol. 6, 2015.

[21] A. Bailey and S. Murray, "Rocket Propellants," in Explosives, Propellant and Pyrotechnics, London, Brassey's, 1989, pp. 99-114.

[22] M. R. Anvekar, "Fundamentals of Rocket Propulsion," in Aircraft Propulsion, PHI, 2016, p. 88.

[23] Y. Aparna, "Synthesis and Characterization of CuO Nano Particles by Novel Sol-Gel Method," in International Conference on Environment Science and Biotechnology, Singapore, 2012.

[24] R. Etefagh, E. Azhir and N. Shahtahmasebi, "Synthesis of CuO nanoparticles and fabrication of nanostructural layer biosensors for detecting Aspergillus niger fungi," Scientia Iranica, vol. 20, no. 3, pp. 1055-1058, 2013.

[25] L. Chen, "Cuo nanocrystals in thermal decomposition of ammonium perchlorate stabilization, structural characterization and catalytic activities," Journal of Thermal Analysis and Calorimetry, vol. 91, no. 2, pp. 581-587, 2008.

[26] G. Mustafa, "Synthesis and characterization of cupric oxide (CuO) nanoparticles and their application for the removal of dyes," African Journal of Biotechnology, vol. 12, no. 47, pp. 6650-6660, 2013.

[27] E. Darezereshki and F. Bakhtiari, "A novel technique to synthesis of tenorite (CuO) nanoparticles from low concentration solution of CuSO4," J. Min. Metall., vol. 47, no. 1, pp. 73-18, 2011.

[28] E. Ayoman, G. Hossini and N. Haghighi, "Synthesis of CuO Nanoparticles and Study on their Catalytic Properties," Int. J. Nanosci. Nanotechnol., vol. 11, no. 2, pp. 63-70, 2015.

[29] P. Srivastava, "Synthesis, characterization and catalytic effect of bimetallic nanocrystals on the thermal decomposition of ammonium perchlorate," IJC, vol. 49, pp. 1339-1344, 2010.

[30] Z.-u.-d. Babar and A. Q. Malik, "Thermal Decom position and Kinetic Evaluation of Composite Propellant Material Catalyzed with Nano Magnesium Oxide,"NUST Journal of Engineering Sciences, vol. 7, no. 1, pp. 5-14, 2014.

[31] B. C. Smith, Fundamentals of Fourier Transform Infrared Spectroscopy, New York: CRC Press, 2011.

[32] R. Sharma, "X-ray diffraction: a powerful method of characterizing nanomaterials," Recent Research in Science and Technology, vol. 4, no. 8, pp. 77-79, 2012.

[33] JEOL, JSM-6490 Series Scanning Electron Microscopes, Tokyo: JEOL Ltd..

[34] V. Ramachandran, Handbook of Thermal Analysis of Construction Materials, NY: Noyes Publications, 2002.

[35] T. Hatakeyama and F. Quinn, Thermal Analysis Fundamentals and Applications to Polymer Science, 2nd ed., West Sussex: John Wiley & Sons Ltd., 1999.

[36] G. Kliche and Z. V. Popovic, "Far-Infrared spectroscopic investigations on CuO," Physical Review B, vol. 42, no. 16, pp. 10061-10066, 1990.

[37] R. D. Aines and G. R. Rossman, "Water in minerals? A peak in the infrared," Journal of Geophysical Research, vol. 89, no. 6, pp. 4059-4071, 1984.